Pergamon

Int. J. Solids Structures Vol. 35, No. 23, pp. 3105–3119, 1998

0020–7683/98 $19.00 + .00

PII: S0020–7683(97)00365–X

THE INFLUENCE OF COUPLING ON THE FREE VIBRATION OF ANISOTROPIC THIN-WALLED CLOSED-SECTION BEAMS

D. STEFAN DANCILA† and ERIAN A. ARMANIOS
Georgia Institute of Technology, Atlanta, Georgia 30322-0150, U.S.A.

(*Received* 18 *June* 1997)

Abstract—A solution procedure for thin-walled laminated composite beams is presented. Two configurations are considered, producing extension-twist and bending-twist coupling, respectively. The influence of coupling on the characteristic equations for free vibration is isolated. It is shown that the characteristic determinant for extension-twist coupling can be expressed as the product of the two decoupled ones. For the case of bending-twist coupling, a simple-quasi-decoupled procedure is developed. This model is shown to provide accurate predictions for natural frequencies of practical interest for slender, laminated composite box beams. © 1998 Elsevier Science Ltd. All rights reserved.

INTRODUCTION

Thin-walled laminated composite beams provide additional flexibility to meet design requirements efficiently. Coupling between deformation modes such as extension, bending and twist can be tailored to produce favorable dynamic response and aeroelastic behavior. From an analytical standpoint, the induced coupling results in additional complexity in the formulation of the governing equations and solution procedures. A theory for the free vibration analysis of anisotropic, thin-walled, closed-section beams was developed by Armanios and Badir (1995). Closed form expressions for the stiffness coefficients and inertia parameters were provided. The governing equations provided by Armanios and Badir (1995) are used in this paper to isolate the influence of coupling on the free vibration of closed section beams exhibiting extension-twist or bending-twist coupling. The objective of this work is to develop a systematic solution procedure that enables the prediction of natural frequencies and mode shapes accurately and efficiently. A comparison between coupled and uncoupled characteristic equations is performed in order to provide further insight into the role of the coupling terms in the solution process. This comparison also leads to the development of a simple, approximate solution methodology that results in accurate prediction of the dynamic response in practical configurations of slender laminated composite box beams.

ANALYTICAL MODEL

The analytical model used in the present investigation has been developed by Armanios and Badir (1995) and, for convenience, a summary of the assumptions, notations and governing equations will be briefly reviewed in the following:

† Author to whom correspondence should be addressed.

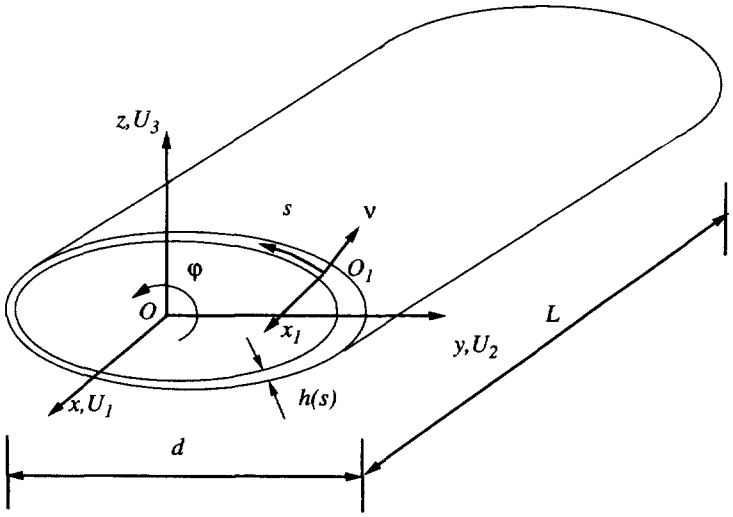

Fig. 1. Coordinate systems and kinematic variables.

Considering a closed-section composite cylindrical shell, illustrated in Fig. 1, it is assumed that the geometric dimensions are such that

$$d \ll L$$
$$h \ll d$$
$$h \ll R \tag{1}$$

where d is an upper bound of the cross sectional dimensions, L is the longitudinal dimension and h is an upper bound on the wall thickness. As a consequence, the shell can be characterized as a slender thin-walled beam. In addition, it is assumed that the variation of the material properties over distances of order d in the axial direction are small relative to their variation in the circumferential direction. The material properties, considered anisotropic, are allowed to vary both in the circumferential and the thickness directions. Finally, the shell thickness itself is allowed to vary along the circumference.

COORDINATE SYSTEM AND KINEMATIC VARIABLES

Global and local coordinate systems are introduced, denoted by $Oxyz$ and O_1x_1vs, respectively, as depicted in Fig. 1. The axis O_1s is defined by the tangent to the midline in the plane of the cross section in a counterclockwise direction, while O_1v is defined by the outward normal to the midline, taken in the same plane. The axis O_1x_1 is taken parallel to Ox. At any point of the cross section, the displacements can be expressed with respect to either coordinate system. Four global kinematic variables are defined at a cross sectional level, denoted as U_1, U_2, U_3 and φ, and representing the averaged displacements along the Ox, Oy and Oz axes and the average cross sectional rotation around the Ox axis, respectively.

CONSTITUTIVE RELATIONSHIPS

A displacement field consistent with a hypothesis of in-plane nondeformabilty of the cross section, but allowing for out-of-plane warping is derived using an asymptotic variational method. The resulting constitutive equations can be expressed as

$$\begin{Bmatrix} T \\ M_x \\ M_y \\ M_z \end{Bmatrix} = \begin{bmatrix} C_{11} & C_{12} & C_{13} & C_{14} \\ C_{12} & C_{22} & C_{23} & C_{24} \\ C_{13} & C_{23} & C_{33} & C_{34} \\ C_{14} & C_{24} & C_{34} & C_{44} \end{bmatrix} \begin{Bmatrix} U_1' \\ \varphi' \\ U_3'' \\ U_2'' \end{Bmatrix} \tag{2}$$

where T, M_x, M_y and M_z represent the axial force, torsional moment and bending moments, respectively. The cross sectional stiffness, denoted by C_{ij}, are formulated in terms of closed form integrals of the material constants and geometry and, for convenience, are provided in Appendix A. The prime associated with the kinematic variables denotes differentiation with respect to x.

EQUATIONS OF MOTION

The equations of motion are obtained using Hamilton's principle. For the case of free vibration, the resulting homogeneous coupled system of equation is:

$$\begin{aligned} C_{11}U_1'' + C_{12}\varphi'' + C_{13}U_3''' + C_{14}U_2''' - m_c\ddot{U}_1 &= 0 \\ C_{12}U_1'' + C_{22}\varphi'' + C_{23}U_3''' + C_{24}U_2''' - I\ddot{\varphi} - S_z\ddot{U}_3 + S_y\ddot{U}_2 &= 0 \\ C_{13}U_1''' + C_{23}\varphi''' + C_{33}U_3'''' + C_{34}U_3'''' + S_z\ddot{\varphi} + m_c\ddot{U}_3 &= 0 \\ C_{14}U_1''' + C_{24}\varphi''' + C_{34}U_3'''' + C_{44}U_2'''' - S_y\ddot{\varphi} + m_c\ddot{U}_2 &= 0 \end{aligned} \tag{3}$$

The coefficients I, Sy, S_z and m_c are also defined in Appendix A based upon material properties, lay-up and cross section characteristics. Superscript dot denotes derivative with respect to time.

PARTICULAR CASES

A closed form solution for the most general case, corresponding to nonzero coupling coefficients in the equations of motion, is not available. However, particular choices of cross sectional shape and lay-up can generate cases of interest in which some of the coefficients vanish. The corresponding form of the equations of motion exhibits fewer coupling terms, allowing a closed form solution. A numerical solution is, of course, an option for all cases.

Two particular configurations, corresponding to specific choices of lay-up have been considered by Armanios and Badir (1995). The first one, designated Circumferentially Uniform Stiffness (CUS), consists of a lay-up that produces the same membrane stiffness coefficients with respect to the local coordinate system at any point of the cross section. The second lay-up is designated Circumferentially AntiSymmetric (CAS). It is characterized by membrane shear coupling stiffness terms that are antisymmetric with respect to the local coordinate system, with all other membrane stiffness terms being symmetric. The symmetry/antisymmetry conditions refer to points on the cross section located at symmetric positions with respect to the plane Oxy.

CIRCUMFERENTIALLY UNIFORM STIFFNESS (CUS)

A typical CUS laminated composite lay-up can be described in the local coordinate system as $[\theta]_n$ along the entire circumference of the cross section. For a rectangular cross section, the CUS lay-up leads to cross sectional properties characterized by

$$C_{13} = C_{14} = C_{23} = C_{24} = C_{34} = 0$$
$$S_y = S_z = 0$$

As a consequence, the equations of motion reduce to

$$C_{11}U_1'' + C_{12}\varphi'' - m_c\ddot{U}_1 = 0$$
$$C_{12}U_1'' + C_{22}\varphi'' - I\ddot{\varphi} = 0$$
$$C_{33}U_3'''' + m_c\ddot{U}_3 = 0$$
$$C_{44}U_2'''' + m_c\ddot{U}_2 = 0$$

which consist to two uncoupled bending equations and a coupled set of equations for extension-twist.

CIRCUMFERENTIALLY ANTISYMMETRIC STIFFNESS (CAS)

An example of a laminated composite lay-up for this case is a combination of $[\theta]_n$ along the cross section top halt, $z > 0$, and $[-\theta]_n$ along the bottom half. The CAS used by Armanios and Badir (1995) consists of $[\theta]_{2n}$ in the top wall, $[-\theta]_{2n}$ in the bottom wall and $[\theta/-\theta]_n$ in the vertical walls. The numerical results presented in the present work are based on this lay-up. The CAS configuration for a rectangular cross section has the following properties

$$C_{12} = C_{13} = C_{14} = C_{24} = C_{34} = 0$$
$$S_y = S_z = 0$$

which reduce the system of equations to

$$C_{11}U_1'' - m_c\ddot{U}_1 = 0$$
$$C_{22}\varphi'' + C_{23}U_3''' - I\ddot{\varphi} = 0$$
$$C_{23}\varphi''' + C_{33}U_3'''' + m_c\ddot{U}_3 = 0$$
$$C_{44}U_2'''' + m_c\ddot{U}_2 = 0$$

where the extension response is uncoupled, as well as the bending about the Oz axis, while the bending about the Oy axis is coupled with twist.

SOLUTION AND RESULTS

The exact solutions for the homogeneous equations of motion corresponding to the free vibration of a cantilevered beam are considered in this work.

CIRCUMFERENTIALLY UNIFORM STIFFNESS (CUS)

The CUS configuration leads to a set of uncoupled equations of motion, corresponding to bending in two orthogonal planes, and a set of two coupled equations of motion for extension-twist. The solution process for the uncoupled bending equations is straightforward. The solution of the coupled set of equations, however, deserves some attention.

Starting from the coupled equations of motion for the extension-twist vibration,

$$C_{11}U_1'' + C_{12}\varphi'' - m_c\ddot{U}_1 = 0$$
$$C_{12}U_1'' + C_{22}\varphi'' - I\ddot{\varphi} = 0$$

and assuming a general solution in the form of

$$U_1(x,t) = \bar{U}_1 e^{\lambda x} e^{i\omega t}$$
$$\varphi(x,t) = \bar{\varphi} e^{\lambda x} e^{i\omega t}$$

one obtains the characteristic equation of the system as

$$(C_{11}C_{22} - C_{12}^2)\lambda^4 + \omega^2(C_{11}I + C_{22}m_c)\lambda^2 + m_cI\omega^4 = 0$$

Denoting

$$a = (C_{11}C_{22} - C_{12}^2)$$
$$b = (C_{11}I + C_{22}m_c)$$
$$c = m_cI$$
$$y = \lambda^2$$

the solutions can be expressed as

$$y_{1,2} = \omega^2 \frac{-b \pm \sqrt{b^2 - 4ac}}{2a}$$

with the understanding that the plus sign is associated with y_1 and the minus with y_2. In the limiting case when $C_{12} \to 0$, it can be observed that, if $C_{11}I > C_{22}m_c$, then

$$y_1 \to -\omega^2 \frac{m_c}{C_{11}}$$
$$y_2 \to -\omega^2 \frac{I}{C_{22}}$$

which indicates that the y_1 root is associated with the axial-mode dominated vibrations, while the y_2 root is associated with the torsionally dominated vibrations. If, on the other hand, $C_{11}I < C_{22}m_c$ the roles are reversed, while if $C_{11}I = C_{22}m_c$, $y_1 = y_2$ and the association can be made either way.

Based on physical considerations, a, b and c are always positive. On the other hand, simple algebra shows that $0 \leqslant (b^2 - 4ac) \leqslant b^2$, which leads to the conclusion that $y_{1,2}$ will both be always real, and $y_{1,2} \leqslant 0$. Therefore, the four roots $\lambda_i = 1, 4$ of the characteristic equations will always be of the form

$$\lambda_{1,2} = \pm i\Lambda_1$$
$$\lambda_{3,4} = \pm i\Lambda_2$$

where

$$\Lambda_{1,2} = \omega \frac{b \mp \sqrt{b^2 - 4ac}}{2a}$$

the minus sign being associated with subscript 1 and the plus sign with subscript 2. The general solution of the system can now be expressed as

$$U_1(x,t) = \{U_{11}\cos(\Lambda_1 x) + U_{12}\sin(\Lambda_1 x) + U_{13}\cos(\Lambda_2 x) + U_{14}\cos(\Lambda_2 x)\}\, e^{i\omega t}$$

$$\varphi(x,t) = \{\varphi_1\cos(\Lambda_1 x) + \varphi_2\sin(\Lambda_1 x) + \varphi_3\cos(\Lambda_2 x) + \varphi_4\cos(\Lambda_2 x)\}\, e^{i\omega t}$$

Imposing cantilevered boundary conditions one obtains the characteristic determinant, expressed as

$$\cos(\Lambda_1 L)\cos(\Lambda_2 L) = 0 \tag{1}$$

which, in turn, leads to

$$\Lambda_{1k} = \frac{(2k+1)\pi}{2L}$$

$$\Lambda_{2k} = \frac{(2k+1)\pi}{2L} \quad k = 0, 1, 2, \ldots$$

The natural frequencies of the system can then be obtained as

$$\omega_{1k} = \frac{(2k+1)\pi}{2L}\sqrt{\frac{2a}{b-\sqrt{b^2-4ac}}}$$

$$\omega_{2k} = \frac{(2k+1)\pi}{2L}\sqrt{\frac{2a}{b+\sqrt{b^2-4ac}}} \qquad k = 0, 1, 2, \ldots$$

or, in a more concise form

$$\omega_k = \frac{(2k+1)\pi}{2L}\sqrt{\frac{2a}{b\mp\sqrt{b^2-4ac}}} \quad k = 0, 1, 2, \ldots$$

Based upon the association we have established between the roots y_1 and y_2, and the type of vibration they correspond to, we now have a criterion for interpreting the signs in the final formula for the natural frequencies. If $C_{11}I > C_{22}m_c$, then the minus sign will generate natural frequencies for the axial-mode dominated vibrations, while the plus sign will generate natural frequencies for torsionally dominated vibrations. Again, if $C_{11}I < C_{22}m_c$ the roles are reversed and if $C_{11}I = C_{22}m_c$, $y_1 = y_2$ and the natural frequencies can be assigned to either type of mode, the values being numerically equal. It is worth noting that eqn (1) is cast as the product of the characteristic equations resulting from the decoupled motions ($C_{12} = 0$). This observation, not generally valid for other cases of coupling, will be discussed in the following for the CAS case.

CIRCUMFERENTIALLY ANTISYMMETRIC (CAS)

The CAS configuration leads to a set of uncoupled and a set of two coupled equations of motion. The uncoupled equations correspond to axial extension and one bending, respectively, while the coupled system describes the bending-twist vibrations.

The solution process for the uncoupled equations is straightforward. The coupled case is discussed in the following.

Starting from the coupled equations of motion for the bending-twist vibration,

$$C_{22}\varphi'' + C_{23}U'''_3 - I\ddot{\varphi} = 0$$

$$C_{23}\varphi''' + C_{33}U''''_3 + m_c\ddot{U}_3 = 0$$

and assuming a general solution in the form of

$$U_3(x,t) = \bar{U}_3\, e^{\lambda x}\, e^{i\omega t}$$

$$\varphi(x,t) = \bar{\varphi}\, e^{\lambda x}\, e^{i\omega t}$$

one obtains the characteristic equation of the system as

$$(C_{22}C_{33} - C_{23}^2)\lambda^6 + \omega^2 C_{33} I\lambda^4 - \omega^2 C_{22} m_c \lambda^2 - m_c I\omega^4 = 0 \tag{2}$$

Denoting

$$a = (C_{22}C_{33} - C_{23}^2)$$

$$b = \omega^2 C_{33} I$$

$$c = \omega^2 C_{22} m_c$$

$$d = \omega^4 m_c I$$

$$y = \lambda^2$$

the equation can be written as

$$ay^3 + by^2 - cy - d = 0 \tag{3}$$

Based on physical considerations, a, b, and c and d are always positive.

The roots of eqn (3) can be expressed in closed form, based upon the values of the coefficients. However, as the expressions are extremely intricate, an attempt to use those roots in a manner similar to that for the CUS case leads to a characteristic determinant that cannot be solved explicitly for ω. Consequently, a closed form solution for the bending-twist vibration cannot be obtained.

The problem will be solved in three ways. While both the first and the second solutions are exact, the first one offers less insight into the characteristics of the system. We therefore choose to present the second one in more detail. The third solution, approximate, uses observations made while developing the second solution to substantiate a simplifying assumption. Numerical solutions for the coupled bending-twist vibration of a CAS cantilevered beam are obtained using a PC-based version of the computer code Mathematica® (Wolfram, 1991). The code allows for both symbolic manipulations and numerical computations with arbitrary precision.

The properties of the cantilevered beam are provided in Table 1.

Table 1. CAS beam properties

Exterior width	24.21 10^{-3} m (0.953 in)
Exterior height	13.46 10^{-3} m (0.537 in)
Length	0.84455 m (33.25 in)
Ply thickness	127 10^{-6} m (0.005 in)
Number of piles	6
E_{11}	142 GPa (20.59 Msi)
$E_{22} = E_{33}$	9.8 GPa (1.42 Msi)
$G_{12} = G_{23}$	6.0 GPa (0.87 Msi)
G_{23}	4.83 GPa (0.7 Msi)
$\nu_{12} = \nu_{13}$	0.42
ν_{23}	0.50
ρ	1601.1 kg/m^3 (1.501 10^{-4} lb s^2/in^4)

SOLUTION I

This solution is more general due to the fact that it does not take into account the specific structure of eqn (2) and its coefficients.

The first step consists of solving for the six roots λ_i, $i = 1, 6$ of the characteristic equation. The solution is carried out by symbolic manipulations, the results being six rather intricate expression. For the general case, these expressions evaluate to complex numbers. The next step consists of expressing the general solution of the system as

$$U_3(x,t) = \{U_{31}\, e^{\lambda_1 x} + U_{32}\, e^{\lambda_2 x} + U_{33}\, e^{\lambda_3 x} + U_{34}\, e^{\lambda_4 x} + U_{35}\, e^{\lambda_5 x} + U_{36}\, e^{\lambda_6 x}\}\, e^{i\omega t}$$

$$\varphi(x,t) = \{\varphi_1\, e^{\lambda_1 x} + \varphi_2\, e^{\lambda_2 x} + \varphi_3\, e^{\lambda_3 x} + \varphi_4\, e^{\lambda_4 x} + \varphi_5\, e^{\lambda_5 x} + \varphi_6\, e^{\lambda_6 x}\}\, e^{i\omega t}$$

Imposing the cantilevered boundary conditions on the solutions and making use of the relationships between U_{3i}, φ_i and λ_i, $i = 1, 6$ stemming from the requirement that the differential equations be identically satisfied, one obtains the characteristic determinant in a symbolic form. The complexities of the expressions involved are prohibitive for hand calculation.

It is not possible to explicitly solve for the roots ω of the characteristic determinant in the above equation. Therefore, a numerical solution is obtained, using predefined procedures available in Mathematica®.

Once a root ω is found, the space-domain eigenvalues λ_i, $i = 1, 6$ and the corresponding singular system matrix are numerically evaluated. A call to a linear system solving procedure then generates the associated eigenvector. A calculation with 50 digit precision overcame numerical difficulties associated with this last step. The resulting components of the eigenvector, representing the coefficients of the various eigenfunctions, can be normalized, and, as a final step, either through direct inspection or by the use of the eigenvectors to generate the animated mode shape one can identify the mode as being bending-dominated or torsion-dominated.

SOLUTION II

This method is a refined version of the previous one. It takes into account the specific structure of the characteristic equation, providing more insight.

Based on Ref. 3, eqn (3) can be reduced to the standard form

$$x^3 + px + q = 0$$

by the substitution

$$y = x - \frac{b}{3}$$

where

$$p = \tfrac{1}{3}(-3c - b^2)$$

$$q = \tfrac{1}{27}(2b^3 + 9bc - 27d)$$

The nature of the solutions can be now identified based upon the sign of the quantity

$$\delta = \frac{q^2}{4} + \frac{p^3}{27}$$

If $\delta < 0$ there are three real and unequal roots; if $\delta = 0$ there are three real roots of which at least two are equal: finally, if $\delta > 0$ there are one real root and two conjugate imaginary roots. However, the expression for δ is intricate and no general statement

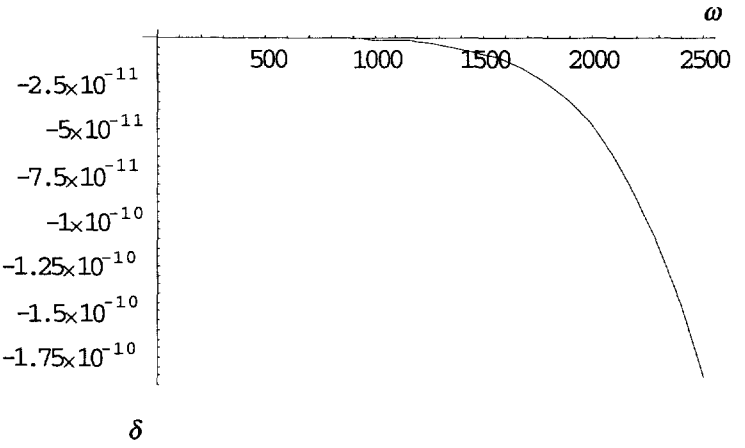

Fig. 2. The variation of δ vs ω, for CAS with $\theta = 30°$.

regarding its sign seems possible. Direct evaluation shows that there exist, generally, combinations of arbitrary numerical values for a, b, c, d and ω for which δ takes either sign. However, restricting the coefficients a, b, c and d to physically meaningful values and plotting the variation of δ vs ω we have always obtained the result $\delta < 0$. A typical plot, corresponding to a fiber angle $\theta = 30°$ is shown in Fig. 2. Therefore, the cubic equation has three real distinct roots and, based upon the signs of the coefficients it follows that they can only be one positive and two negative. The roots for this case are

$$x_k = 2\sqrt{-\frac{p}{3}}\cos\left(\frac{\Phi}{3} + \frac{2k\pi}{3}\right)$$

where

$$\cos\Phi = \mp\sqrt{\frac{q^2/4}{-p^3/27}}$$

and the minus sign is to be used if q is positive and the plus otherwise.

The roots λ_i, $i = 1, 6$ will result, therefore, as $\pm ik_1$, $\pm ik_2$ and $\pm k_3$, respectively, and the general solution of the coupled system can be expressed as

$$\begin{aligned} U_3(x,t) = {} & \{U_{31}\sin(k_1x) + U_{32}\cos(k_1x) + U_{33}\sin(k_2x) + U_{34}\cos(k_2x) \\ & + U_{35}\sinh(k_3x) + U_{36}\cosh(k_3x)\}\, e^{i\omega t} \\ \varphi(x,t) = {} & \{\varphi_1\sin(k_1x) + \varphi_2\cos(k_1x) + \varphi_3\sin(k_2x) + \varphi_4\cos(k_2x) \\ & + \varphi_5\sinh(k_3x) + \varphi_6\cosh(k_3x)\}\, e^{i\omega t} \end{aligned}$$

One important remark at this point is that for all the combinations of beam cross-sectional properties investigated, k_3 and one of k_1 or k_2, depending upon the choice of subscript assignment, have almost identical values over a considerable range of ω. This behavior is illustrated in Fig. 3, where k_2 is very close to k_3 for a range of ω of up to 20,000 rad/s. This observation will be used in the development of the approximate solution.

Imposing the cantilevered boundary conditions on the solutions and making use of the relationships between U_{3i}, φ_i and λ_i, $i = 1, 6$ stemming from the requirement that the differential equations be identically satisfied, one obtains the characteristic determinant in a symbolic form, which can be reduced to

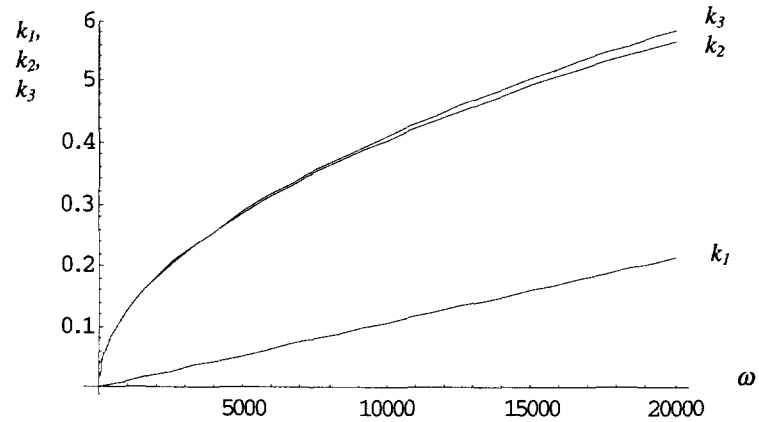

Fig. 3. Variation of k_1, k_2 and k_3 vs ω.

$$\Delta(k_1, k_2, k_3) = 0 \tag{4}$$

The expression for $\Delta(k_1, k_2, k_3)$, provided in Appendix B, does not explicitly depend upon ω.

The characteristic determinant, however, cannot be solved in a manner similar to the case of an isotropic cantilevered beam, where it reduces to

$$\cos(kL)\cosh(kL) = -1$$

for bending vibrations and it is expressed by one of the terms in eqn (1) for axial and twisting vibrations. The fundamental difference is that the solutions to eqn (4) form, in principle, a double infinity of triplets (k_1, k_2, k_3). Of all the triplets, only the ones that simultaneously generate the six roots of eqn (2), $\lambda_{1,2} = \pm ik_1$, $\lambda_{3,4} = \pm ik_2$ and $\lambda_{5,6} = \pm k_3$ corresponding to some real value ω, should be retained.

A numerical solution, using a predefined root finding routine is chosen. Plotting the determinant value, in this case a real number, vs ω allows one to bracket each successive root in an interactive manner.

From this point the solution follows the steps described in the previous section. As expected, the results obtained by using either solution are the same.

As an illustration of this method, we expand on the CAS example of Armanios and Badir (1995), by computing the natural frequencies of free vibration as a function of the lay-up angle parameter, θ. The numerical values are provided in Table 2 and plotted in

Table 2. CAS natural frequencies, in Hz

Ply Angle, degrees	B1	B2	B3	B4	B5	B6	B7	B8	T1	T2
0	43.76	274.22	767.83	1504.63	2487.27	3715.55	5189.49	6909.08	483.17	1449.51
15	30.57	191.10	532.73	1040.05	1700.65	2520.02	3458.09	4559.52	701.76	2113.63
30	19.92	124.74	348.74	681.56	1124.55	1673.71	2323.84	3083.68	862.68	2593.55
45	14.69	92.03	257.56	504.35	833.49	1243.28	1733.91	2302.39	782.42	2352.00
60	12.52	78.43	219.59	430.23	711.14	1061.96	1482.69	1970.85	660.07	1983.03
75	11.70	73.30	205.25	402.20	664.85	993.12	1387.01	1846.53	557.98	1673.97
90	11.49	72.01	201.64	395.14	653.19	975.75	1362.83	1814.41	483.17	1449.51

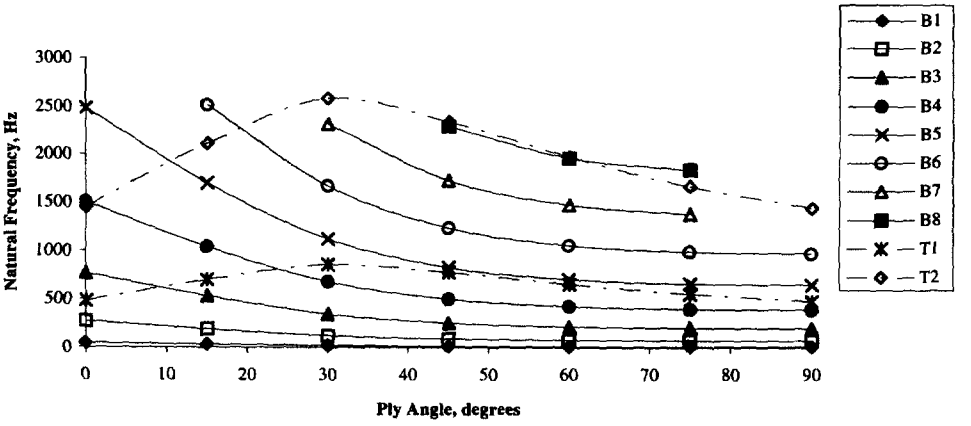

Fig. 4. CAS Natural Frequencies vs ply angle.

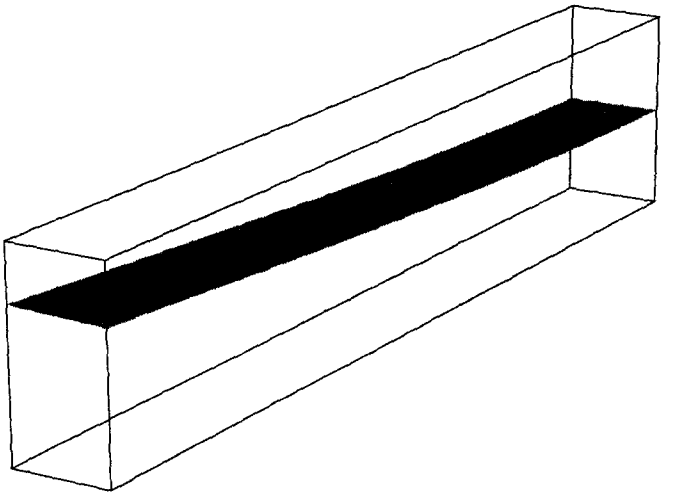

Fig. 5. Mode shape B1 for CAS, $\theta = 30^{\circ}$.

Fig. 4. The symbols B1–B8 denote bending-dominated modes, whereas T1 and T2 denote twisting-dominated modes. For lower modes, both the numerical values of the eigenvectors and the animated mode shape allow a clear identification of the dominant component. For higher modes, however, both types of deformation can be recognized as having similar contribution. This is illustrated for $\theta = 30^{\circ}$ where the mode shapes associated with B1, B5 and T1 appear in Figs 5–7 by plotting the midplane displacements. While Figs 5 and 7 show dominant first bending and twisting deformations, respectively, the fifth bending mode (Fig. 6) is highly coupled.

SOLUTION III

This approximate solution is based upon the previous observation regarding the variation of k_1, k_2 and k_3. If one substitutes k_3 for k_2 in eqn (4), the results is

$$-2k_3^4(k_3^4 - k_1^4)\cos(k_1 L)[1 + \cos(k_3 L)\cosh(k_3 L)] = 0$$

It follows that either

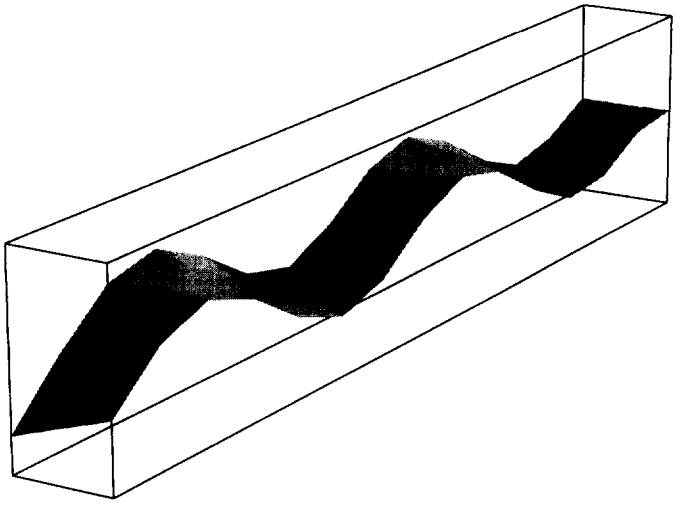

Fig. 6. Mode shape B5 for CAS, $\theta = 30°$.

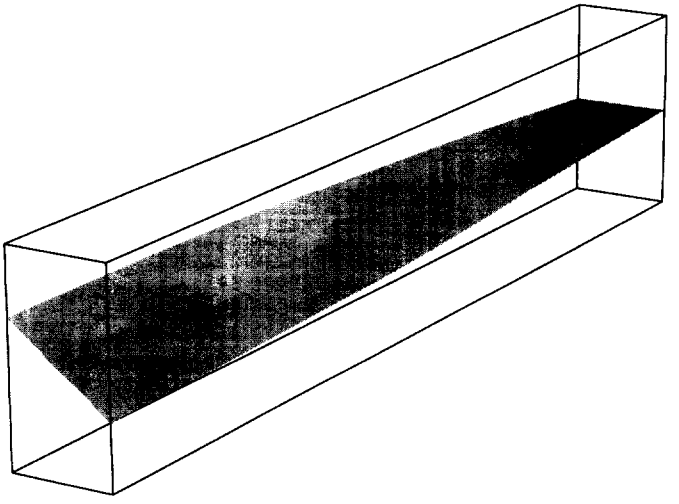

Fig. 7. Mode shape T1 for CAS, $\theta = 30°$.

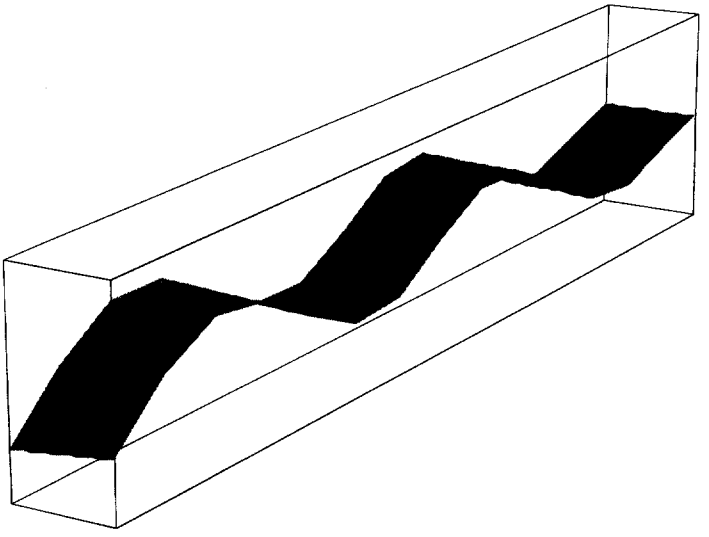

Fig. 8. Mode shape B5 for CAS, $\theta = 30°$, long beam.

Table 3. Comparison of approximate and exact natural frequency solutions for CAS, $\theta = 30^{\circ}$

	Exact solution, Hz	Approximate solution, Hz	Percentage difference
B1	19.92	19.92	0.00%
B2	124.74	124.95	0.17%
T1	862.68	861.68	−0.12%
T2	2593.55	2586.69	−0.26%

$$k_1 = \frac{(2m+1)\pi}{2L} \quad m = 0, 1, 2, \ldots$$

or k_3 is a solution of the beam bending equation

$$\cos(k_3 L)\cosh(k_3 L) = -1$$

for which the first few numerical solutions are well-known. From this observation it follows that for this case an approximate solution could be cast as the product of decoupled bending and twisting behavior.

Solving eqn (2) for ω results in

$$\omega^2 = \frac{-(C_{22}m_c\lambda^2 - C_{33}I\lambda^4)}{2m_cI} \pm \frac{\sqrt{(C_{22}m_c\lambda^2 - C_{33}I\lambda^4)^2 + 4m_cI(C_{22}C_{33} - C_{23}^2)\lambda^6}}{2m_cI} \tag{5}$$

By substituting $\lambda = \pm ik_1$, and $\lambda = \pm k_3$ into eqn (5) and using only the plus sign the approximate values of the natural frequencies of the system are obtained. A comparison of the frequencies B1, B2, T1 and T2 with the results from Table 2 and the associated percentage differences appear in Table 3. This indicates that, at least for a range of parameters of practical interest, the quasi-decoupled model corresponding to $k_2 = k_3$ yields excellent results. The characteristic determinant in this case is similar to the CUS and could be constructed as the product of the uncoupled bending and twisting characteristic determinants.

FINITE ELEMENT VALIDATION

In order to validate the accuracy of the procedure proposed for the CAS case, a comparison with finite element results was performed for a slender, thin-walled beam in a cantilevered configuration. The cross sectional, lay-up and material properties of the beam considered were identical with the ones used in the previous section. The length of the beam, however, was increased to a value of 4 m in order to ensure compliance with the assumptions in eqn (1).

The finite element analysis has been conducted by using the code ABAQUS, with the beam modeled by using 900 rectangular reduced integration shell elements of the type designated S4R.

The first six natural frequencies of free vibration obtained by the two methods are compared in Table 4 as a function of the lay-up angle parameter, θ. The agreement between the two sets of predictions is excellent. The symbols B1–B6 denote bending-dominated modes, where T1 denotes twisting-dominated mode. For all modes, the numerical values of the eigenvectors and the animated mode shapes, in the case of the proposed procedure, as well as the graphical representation of mode shapes, in the case of the finite element analysis, allow a clear identification of the dominant component. By comparison with the shorter beam, studied in previous sections, it was observed that the amount of coupled deformation shown by corresponding mode shapes decreases. This can be observed by

Table 4. Comparison of CAS natural frequencies, in Hz

Ply Angle, degrees	Analysis	B1	B2	B3	B4	B5	B6	T1
0	Analytical	1.95	12.22	34.23	67.07	110.88		102.30
	ABAQUS	1.92	12.05	33.67	65.77	108.27		102.13
15	Analytical	1.36	8.54	23.91	46.85	77.42	115.6	
	ABAQUS	1.34	8.39	23.53	46.20	76.58	114.77	
30	Analytical	0.89	5.57	15.58	30.54	50.47	75.39	
	ABAQUS	0.87	5.46	15.33	30.13	50.00	75.08	
45	Analytical	0.65	4.10	11.49	22.52	37.22	55.60	
	ABAQUS	0.65	4.05	11.35	22.31	37.03	55.61	
60	Analytical	0.56	3.50	9.79	19.19	31.72	47.37	
	ABAQUS	0.55	3.47	9.73	19.12	31.74	47.66	
75	Analytical	0.52	3.27	9.15	17.93	29.64	44.28	
	ABAQUS	0.51	3.26	9.13	17.95	29.78	44.71	
90	Analytical	0.51	3.21	8.99	17.61	29.11	43.50	
	ABAQUS	0.51	3.20	8.98	17.65	29.29	43.96	

comparing the mode shape B5 for the long beam, for $\theta = 30^\circ$, represented in Fig. 8, with its counterpart for the short beam, represented in Fig. 6. The comparison suggests that for a given set of values for cross-sectional beam stiffnesses the effect of coupling on mode shapes decreases with the increase in beam length.

CONCLUSIONS

A solution procedure has been developed for the prediction of natural frequencies and mode shapes of slender thin walled laminated composite beams. The influence of coupling on the response of laminated composite box beams with extension-twist or bending-twist coupling has been presented. Of significance is the development of a simple quasi-decoupled solution procedure that provides accurate predictions of natural frequencies with little computational effort. A comparison with results from a finite element analysis validates the proposed procedure. The comparison of two beams of identical cross section, material characteristics and lay-up and different lengths suggests that the effect of coupling on the mode shapes decreases with beam length.

Acknowledgements—This work was supported by the U.S. Army Research Office under Grant DAAL03-92-G-03A0. This support is gratefully acknowledged. The authors would like to also acknowledge Mr Cameron Coates' assistance in performing the finite element calculations.

REFERENCES

Armanios, E. A. and Badir, A. M. (1995) Free vibration analysis of anisotropic thin-walled closed-section beams. *AIAA Journal* **33**, 1905–1910.

Burrington, R. S. (1972) *Handbook of Mathematical Tables and Formulas*, 5th ed, pp. 12–14. McGraw-Hill Book Company.

Wolfram, S. (1992) *Mathematica*, 2nd ed. Addison-Wesley Publishing Company.

APPENDIX A

The closed form expressions for the stiffness coefficients in eqn (2) are:

$$C_{11} = \oint\left(A - \frac{B^2}{C}\right)ds + \frac{(\oint(B/C)\,ds)^2}{\oint(1/C)\,ds} \quad C_{12} = \frac{\oint(B/C)\,ds}{\oint(1/C)\,ds}A_c$$

$$C_{13} = -\oint\left(A - \frac{B^2}{C}\right)z\,ds - \frac{\oint(B/C)\,ds\oint(B/C)z\,ds}{\oint(1/C)\,ds} \quad C_{14} = -\oint\left(A - \frac{B^2}{C}\right)y\,ds - \frac{\oint(B/C)\,ds\oint(B/C)y\,ds}{\oint(1/C)\,ds}$$

$$C_{22} = \frac{1}{\oint(1/C)\,ds} A_e^2 \quad C_{23} = -\frac{\oint(B/C)z\,ds}{\oint(1/C)\,ds} A_e \quad C_{24} = -\frac{\oint(B/C)y\,ds}{\oint(1/C)\,ds} A_e \quad C_{33} = \oint\left(A - \frac{B^2}{C}\right) z^2\,ds + \frac{(\oint(B/C)z\,ds)^2}{\oint(1/C)\,ds}$$

$$C_{34} = \oint\left(A - \frac{B^2}{C}\right) yz\,ds - \frac{\oint(B/C)y\,ds \oint(B/C)z\,ds}{\oint(1/C)\,ds} \quad C_{44} = \oint\left(A - \frac{B^2}{C}\right) y^2\,ds - \frac{(\oint(B/C)y\,ds)^2}{\oint(1/C)\,ds}$$

where

$$A(s) = A_{11} - \frac{(A_{12})^2}{A_{22}} \quad B(s) = 2\left[A_{16} - \frac{A_{12}A_{16}}{A_{22}}\right] \quad C(s) = 4\left[A_{66} - \frac{(A_{26})^2}{A_{22}}\right]$$

and A_{ij} are the membrane, in-plane stiffnesses of the laminate and A_e represents the area enclosed by the midline of the cross section. The inertia-related coefficients are given by

$$m_c = \oint \rho h(s)\,ds \quad I = \oint \rho(y^2+z^2)h(s)\,ds \quad S_y = \oint \rho z h(s)\,ds \quad S_z = \oint \rho y h(s)\,ds$$

with $h(s)$ representing the wall thickness and ρ the material density.

APPENDIX B

Reduced form of the characteristic determinant for the CAS configuration:

$$\begin{aligned}\Delta(k_1,k_2,k_3) = {} & 2k_1^2k_3^2(k_2^4-k_3^4)(k_1^4-k_2^4)\cos(k_2L) + 2k_2^2k_3^2(k_3^4-k_1^4)(k_1^4-k_2^4)\cos(k_1L) \\ & + 2k_1^2k_2^2(k_2^4-k_3^4)(k_1^4-k_3^4)\cosh(k_3L) + k_1k_2(k_1^2+k_2^2)(k_1^4-k_3^4)(k_3^4-k_2^4)\sin(k_1L)\sin(k_2L)\cosh(k_3L) \\ & + k_1k_3(k_1^4-k_2^4)(k_3^2-k_1^2)(k_2^4-k_3^4)\sin(k_1L)\cos(k_2L)\sinh(k_3L) \\ & + k_2k_3(k_2^4-k_1^4)(k_3^2-k_2^2)(k_1^4-k_3^4)\cos(k_1L)\sin(k_2L)\sinh(k_3L) \\ & - [k_1^4k_2^4(k_1^4+k_2^4+2k_3^4) - k_2^4k_3^4(k_2^4+k_3^4-2k_1^4) + k_1^4k_3^4(k_1^4-k_3^4+2k_2^4)]\end{aligned}$$